AD-A265 681

ENTATION PAGE

Form Approved
OBM No. 0704-0188

(2)

rt Date.	3. Report Type and Dates Covered. Final - Journal Article

4. Title and Subtitle.
Finding Mesoscale Ocean Structures with Mathematical Morphology

5. Funding Numbers.

Contract	
Program Element No	0602435N
Project No.	3582
Task No	MOG
Accession No	DN256010
Work Unit No.	13212R

6. Author(s).
Suzanne M. Lea* and Matthew Lybanon

7. Performing Organization Name(s) and Address(es).
Naval Research Laboratory
Remote Sensing Applications Branch
Stennis Space Center, MS 39529-5004

8. Performing Organization Report Number.
JA 321:047:92

9. Sponsoring/Monitoring Agency Name(s) and Address(es).
Naval Research Laboratory
Exploratory Development Group
Stennis Space Center, MS 39529-5004

10. Sponsoring/Monitoring Agency Report Number.
JA 321:047:92

11. Supplementary Notes.
Published in Remote Sensing Environment.
*The University of North Carolina at Greensboro

12a. Distribution/Availability Statement.
Approved for public release; distribution is unlimited.

12b. Distribution Code.

13. Abstract *(Maximum 200 words).*

We introduce a technique to aid in interpreting infrared satellite images of the North Atlantic Ocean Gulf Stream region. Present interpretive methods are largely manual, require significant effort, and are highly dependent on the interpreter's skill. Our quasiautomated technique is based on mathematical morphology, specifically the image transformations of opening and closing, which are defined in terms of erosion and dilation. The implementation performs successive openings and closings at increasing thresholds until a stable division into objects and background is found. This method finds the North Wall of the Gulf Stream in approximately the same place as human analysts and another automated procedure, and does less smoothing of small irregularities than the other two methods. The North Wall is continuous and sharp except where obscured by clouds. Performance in locating warm-core eddies is also comparable to the other methods. However, the present procedure does not find cold-core rings well. We are presently investigating ways to reduce the effects of clouds and delete the unwanted water areas found by the method. We expect to be able to improve the cold-core eddy performance.

93-13152

14. Subject Terms.
Remote sensing, artificial intelligence, data assimilation, satellite data

15. Number of Pages.
9

16. Price Code.

17. Security Classification of Report.	18. Security Classification of This Page.	19. Security Classification of Abstract.	20. Limitation of Abstract.
Unclassified	Unclassified	Unclassified	SAR

DISCLAIMER NOTICE

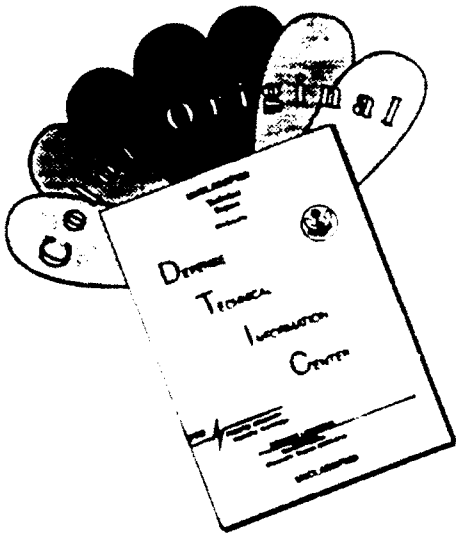

THIS DOCUMENT IS BEST QUALITY AVAILABLE. THE COPY FURNISHED TO DTIC CONTAINED A SIGNIFICANT NUMBER OF COLOR PAGES WHICH DO NOT REPRODUCE LEGIBLY ON BLACK AND WHITE MICROFICHE.

REMOTE SENS. ENVIRON. 44:25–33 (1993)

Finding Mesoscale Ocean Structures with Mathematical Morphology

Suzanne M. Lea
Department of Mathematics, The University of North Carolina at Greensboro

Matthew Lybanon
Remote Sensing Branch, Naval Research Laboratory, Stennis Space Center

We introduce a technique to aid in interpreting infrared satellite images of the North Atlantic Ocean Gulf Stream region. Present interpretive methods are largely manual, require significant effort, and are highly dependent on the interpreter's skill. Our quasiautomated technique is based on mathematical morphology, specifically the image transformations of opening and closing, which are defined in terms of erosion and dilation. The implementation performs successive openings and closings at increasing thresholds until a stable division into objects and background is found. This method finds the North Wall of the Gulf Stream in approximately the same place as human analysts and another automated procedure, and does less smoothing of small irregularities than the other two methods. The North Wall is continuous and sharp except where obscured by clouds. Performance in locating warm-core eddies is also comparable to the other methods. However, the present procedure does not find cold-core rings well. We are presently investigating ways to reduce the effects of clouds and delete the unwanted water areas found by the method. We expect to be able to improve the cold-core eddy performance.

Address correspondence to Matthew Lybanon, Remote Sensing Branch, Naval Research Lab., Stennis Space Center, MS 39529-5004.

Received 27 March 1992; revised 27 June 1992

0034-4257/93/$6.00

655 Avenue of the Americas, New York, NY 10010

INTRODUCTION

Infrared satellite images of the ocean provide surface temperature measurements which can be used either to supplement local measurements at various depths obtained by conventional oceanographic techniques or to provide information about areas of the ocean where data from conventional techniques is sparse. Figure 1 shows a sample infrared image of the Gulf Stream area of the Atlantic Ocean. Bright areas in this image correspond to low temperatures, either of the ocean surface or of clouds.

The Gulf Stream transports tropical water and heat over large distances, and drives many physical processes in the Atlantic. Areas of closed circulation (vortices) near the Gulf Stream, called rings or eddies, form part of the Gulf Stream system. The Gulf Stream and its associated eddies are examples of mesoscale (50–300 km in size) ocean features.

Presently, interpretation of satellite ocean images is performed largely by humans. Consequently, interpretation is a lengthy and laborious process, as well as subjective in nature and highly dependent on the interpreter's skill. To address this problem, an automated system is being developed to interpret mesoscale features for these images. The system, or components of it, are described by Lybanon et al. (1986), Krishnakumar

Figure 1. An original image of the Gulf Stream area of the Atlantic Ocean from NOAA-9. The image is a warmest-pixel composite of images acquired 7–8 March 1987. Bright areas in the image correspond to low temperatures. The image is displayed using histogram equalization to enhance the contrast.

et al. (1990), and Lybanon et al. (1990). This system divides the problem into four parts: segmentation, feature labeling, feature synthesis, and mesoscale extrapolation.

The segmentation portion of the system presently consists of edge detection using the grey-level cooccurrence matrix, as described by Holyer and Peckinpaugh (1989; Peckinpaugh and Holyer, 1991). Cayula et al. (1991) compare that method with another. Cambridge (1991) and Lybanon et al. (1990) discuss incorporation of region detection into this stage (see also Haddon and Boyce, 1990). The feature labeling process uses a relaxation labeling technique due to Krishnakumar et al. (1990), and Krishnakumar and Iyengar (1991); the use of genetic algorithms is also being investigated, as described by Buckles and Petry (1991). Feature synthesis combines discontinuous labeled edges into continuous features, such as a normal mode reconstruction of the Gulf Stream's North Wall, presented by Molinelli and Flanigan (1987). [Molinelli et al. (1991) also discuss the use of neural networks to synthesize North Walls.] The mesoscale extrapolation module uses an expert system to predict kinematically the motion of eddies, since numerical models based on physical principles cannot yet predict eddy motion well. The latter problem is discussed by Lybanon and Thompson (1991), and Lybanon et al. (1990).

The present work is relevant to the segmentation and synthesis portions of the system. This article discusses the use of mathematical morphology to find eddies and the North Wall of the Gulf Stream. Previous work in this area had used primarily statistical pattern recognition techniques and decision theory [see Haralick (1982); later work appears in Gerson et al. (1982), Coulter (1983), Janowitz (1985), and Nichol (1987).] Szczechowski (1991) discusses using the Marr-Hildreth operator to detect eddies.

DATA AND PROCESSING

Infrared images of the Gulf Stream area of the Atlantic Ocean are obtained from Channel 4 (10.3–11.3 μm) of the Advanced Very High Resolution Radiometer (AVHRR) aboard the NOAA-9 and NOAA-11 satellites. This instrument produces 2048 10-bit samples per scan line in each channel. The resulting images are processed to 512×512 pixels with 8 bits of intensity. They are 512×512-pixel sections with a pixel size of 2.5 km. The 8-bit intensity range covers the temperature range of interest with the instrument's full thermal resolution. The images used in the study are warmest-pixel composites of two or more consecutive images, to reduce cloud cover.

The algorithm used to find eddies and the North Wall of the Gulf Stream is based on the image transformations of opening and closing developed by Serra (1982) in connection with texture analysis of digital images. Useful reviews and discussions may be found in Haralick et al. (1987) and Wilson (1989). A complete description of this algorithm and its implementation for astronomical images is given by Lea and Kellar (1989). Lea (1991) discusses adaptations of the algorithm required for its use with infrared satellite images of oceans; these adaptations are summarized below.

The operations of opening and closing are defined in terms of the familiar erosion and dilation operations. The operations can best be understood by considering a single row of an image (Fig. 2). The structure element (a 3-pixel-wide rectangle, in this case) slides along the line, with

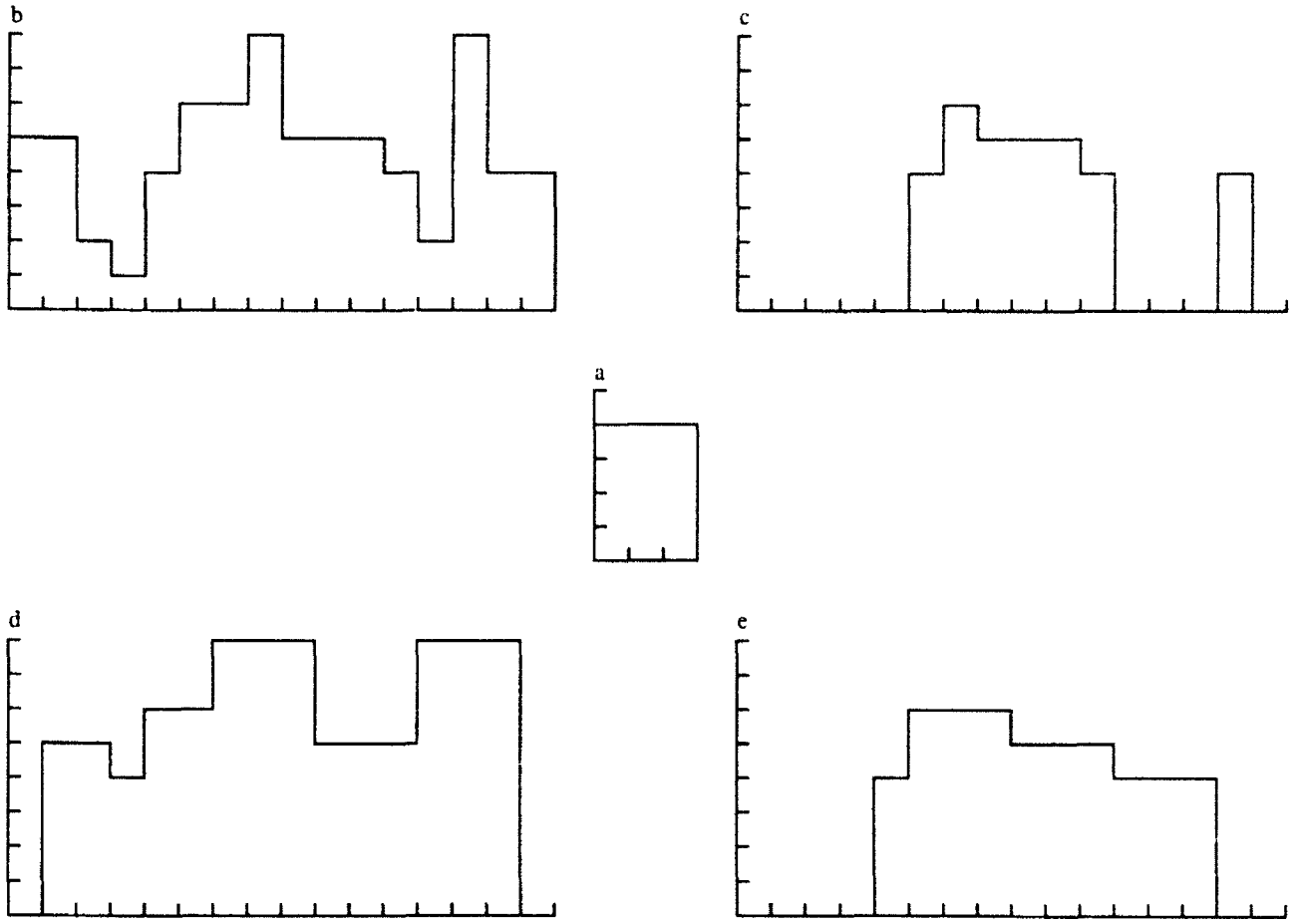

Figure 2. The erosion and dilation operations. a) The structure element is the rectangle 3 pixels wide by 4 intensity units high. b) One line of an image 16 pixels wide is displayed. The structure element slides along this line, as discussed in the text. c) The resulting eroded image (see text). d) The resulting dilated image (see text). e) The resulting opened and closed image (see text).

its center corresponding successively to pixels 2–15 of the image. For erosion, when the entire rectangle fits under or at the image intensity line, the pixel in the transformed image corresponding to the center pixel of the rectangle is given the minimum intensity of the pixel and its two neighbors in the original image; otherwise, the pixel is set to zero intensity. (A structure element having odd width n would be compared to $n-1$ neighbors.) For dilation, if any pixel of the rectangle fits under or at the image intensity line, the corresponding center pixel is given the maximum intensity of the pixel and its two neighbors in the original image; otherwise, the pixel is set to zero intensity. In three dimensions, the rectangle becomes a box, and there are eight neighbors to be considered in determining the minimum or maximum. Structure elements of size larger than 3×3 may be used, but the 3×3 size gives the smoothest edges on the images used.

An opening is an erosion followed by a dilation of the eroded image. A closing is a dilation followed by an erosion of the dilated image. The implementation opens the image and then closes the opened image at a particular threshold (box height). The output of this step is the input to the next step, opening and closing at a higher threshold. The process is repeated until a stable division into objects and background has been found. The division is considered stable when no pixels change classification (from object to background or the reverse) between the beginning of an opening and closing step and its end.

The implementation will not find eddies directly in the ocean images for three reasons: First, the implementation expects to find bright objects

against a dark background; second, it expects to find objects which are uniform or increase in intensity toward their centers; and third, it expects to find (or reject) the brightest objects in the image. (In other words, the implementation was originally designed to find stars in astronomical images.) Although it might be preferable to adjust the algorithm to find eddies directly, doing so would require knowing the approximate intensity range of the eddies before processing. Acquiring this information, however, requires finding the eddies themselves. Fortunately, preprocessing the NOAA images makes use of the existing implementation possible.

The initial preprocessing step is to invert the image, so that regions of high intensity correspond to hot objects. Since the opening and closing operations are used to remove both very hot and cold objects, it might seem that this step is unnecessary; in practice, however, the implementation finds warm-core eddies more reliably if the images are inverted. This increased reliability is ascribed to the fact that warm-core eddies look more like stars in inverted images.

After image inversion, the opening and closing operations are used to find and remove very hot objects (usually land and the Gulf Stream). Operation of this stage of the processing is speeded up by starting the iteration at a relatively large intensity threshold. An estimate of its value can be determined from the unprocessed image:

$$t = 120.7(m/255) + 0.30a - 2n, \qquad (1)$$

where t is the threshold, m is the largest intensity present in the image, a is the average image intensity, and n is the average of the square roots of the intensities. [The coefficients of m and a in Eq. (1) may vary with season; the equation is a multivariate least-squares fit to the set of test images, which were mostly obtained during April and May.] For best results, the criterion for separating objects from background needs to be relaxed. Exactly two iterations are performed; if 0.2% or more, but fewer than 1.0% of the pixels are still changing classification, a new threshold is estimated from the visual results, and two iterations are done starting at that value. This process is repeated until the results are satisfactory. Some pixels remain ambiguously classified as a consequence of using only two iterations; however, in the images studied, 99.3–99.8% of the pixels are unambiguously classified as a result of this procedure.

In the output image, pixels in objects found are set to 0 intensity, and pixels in the background have their intensities set to the value in the original image. Ambiguous pixels are assigned to whatever category they happen to occupy at the time the iteration is stopped. The behavior of the algorithm at the edges of objects causes a 1-pixel-wide border to be discarded from this output image.

The output image from the previous processing step is used as the input image for the final processing step. In this step, the opening and closing operations are used again, with both a smaller increment and a smaller initial threshold (since the brightest objects have been removed), to separate remaining hot objects from the colder background and remove the background. Operation of this stage of the processing is speeded up both by keeping only sizable objects (e.g., 25×25) and by starting the iteration at a nonzero intensity threshold. The value of this threshold can be estimated from the output images of the first step:

$$t = 132.6(m/255) - 0.36a - 2n. \qquad (2)$$

[Equation (2), like Eq. (1), is a multivariate least-squares fit to the set of output images resulting from performing the first processing step on the set of test images. Consequently, the coefficients of m and a may vary with season here also.] The relaxed criterion for separating objects from background is used here as well.

In the output image from this step, pixels in objects are assigned the intensity of the original image, and pixels in the background are assigned intensity values of 0. Ambiguous pixels again are assigned to whatever category they occupy at the time the iteration stops. A 1-pixel-wide border is also removed from this output image.

RESULTS AND DISCUSSION

Figures 3–6 show the results of using the implementation on various images. In each case, image a is the original (inverted) image, image b is image a with bright objects removed, showing the North Wall of the Gulf Stream, and image c is image b with cold objects removed. Image d (if present) shows, for comparison, the results of a human analysis and another automated analysis. The lat-

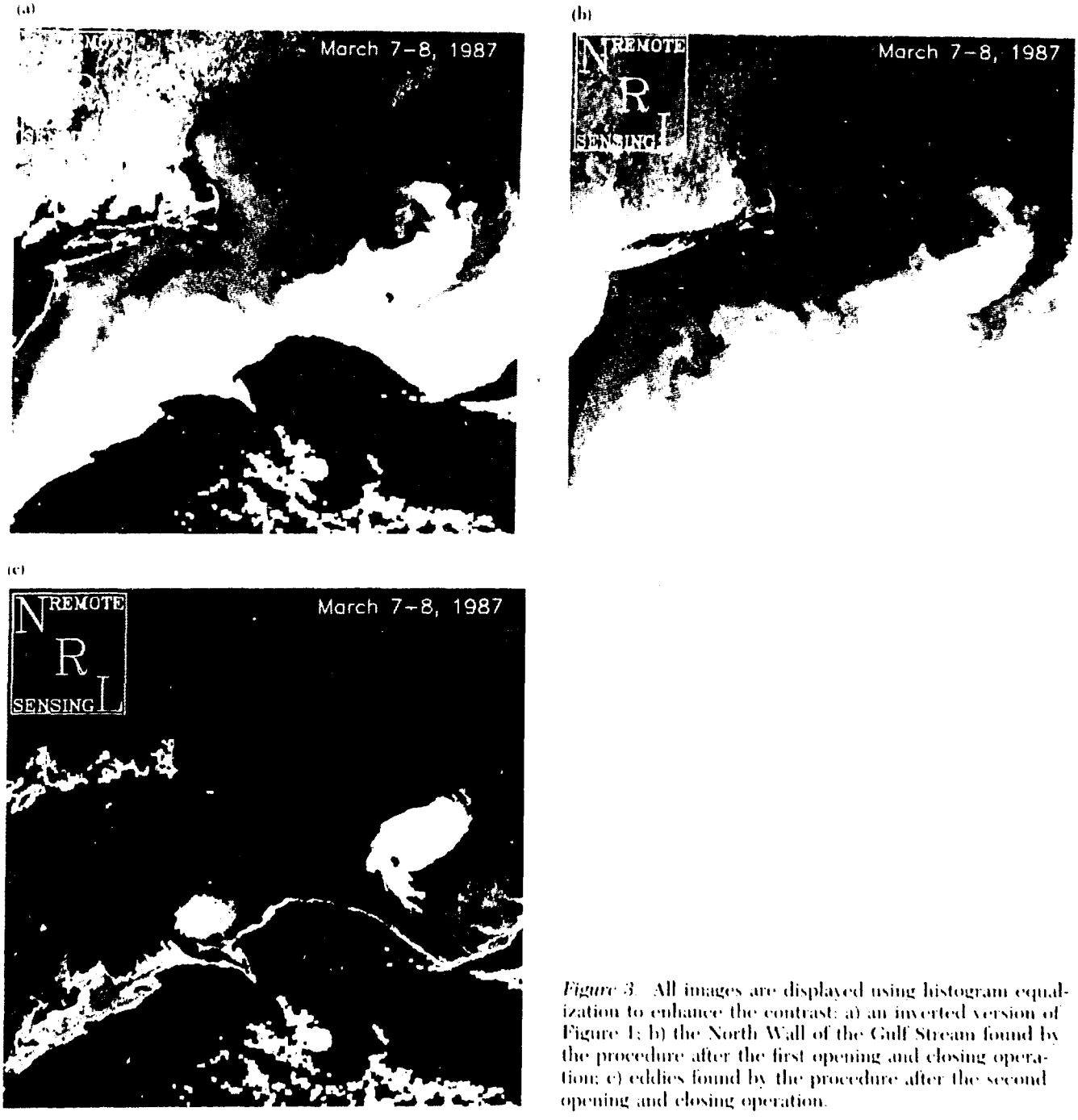

Figure 3. All images are displayed using histogram equalization to enhance the contrast: a) an inverted version of Figure 1; b) the North Wall of the Gulf Stream found by the procedure after the first opening and closing operation; c) eddies found by the procedure after the second opening and closing operation.

ter is described by, for example, Lybanon et al. (1990). All images are displayed using histogram equalization, to reduce loss of contrast in the reproduction process.

Figure 3a shows an inverted composite image from 7–8 March 1987. This image is unusually free from cloud cover. The North Wall appears clearly in Figure 3b, and the warm-core eddies found are shown in Figure 3c. The eddies are attached to unwanted trails of water in this image. The implementation can remove most of these trails, but only at the cost of specializing the thresholds to the particular image.

Figure 4a shows an inverted composite image from 10–12 April 1989. This image has rather a large amount of cloud cover present. The North Wall appears clearly in Figure 4b except where clouds actually obscure it. The procedure does

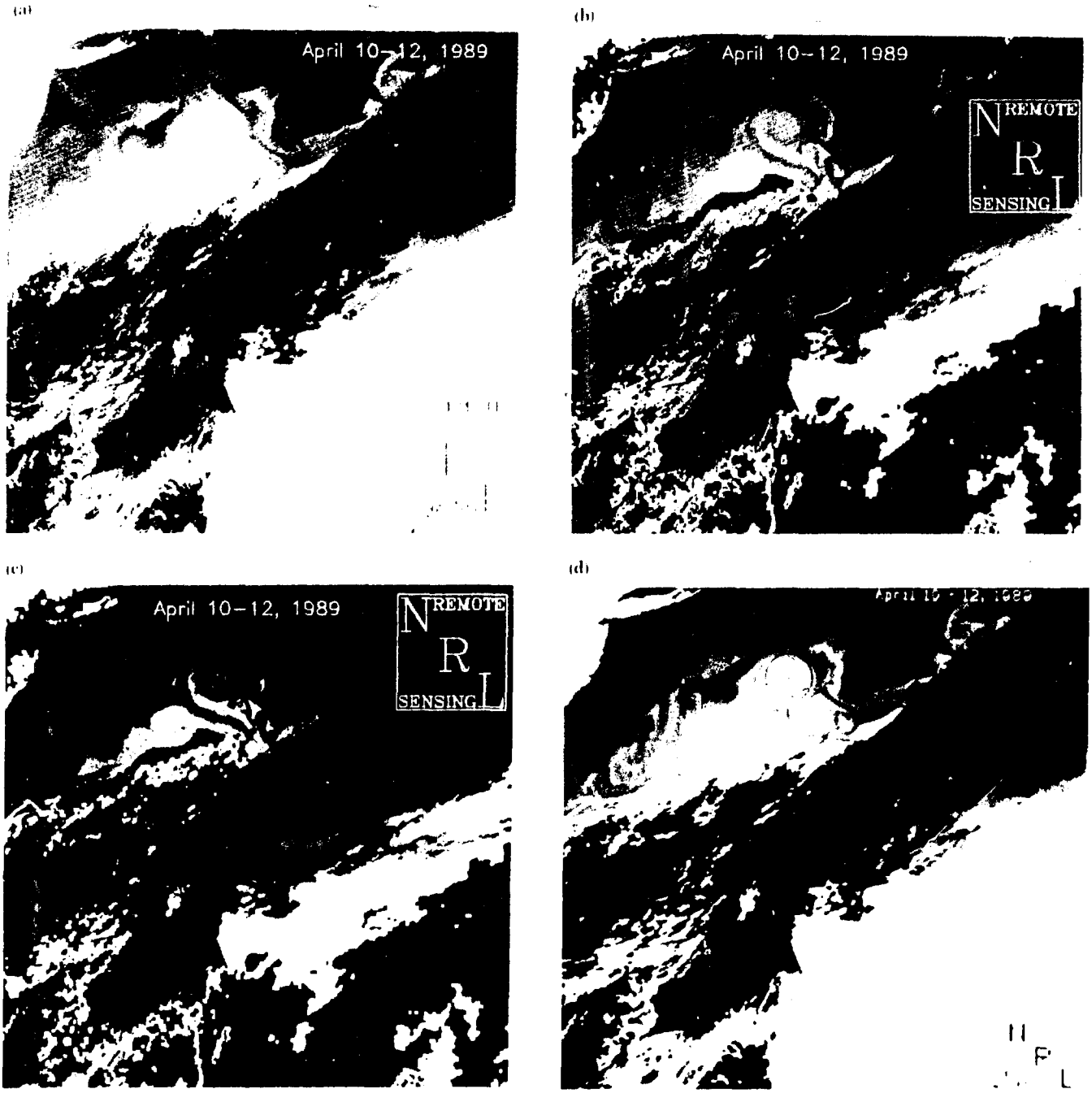

Figure 4. All images are displayed using histogram equalization to enhance the contrast: a) an inverted warmest-pixel composite of images acquired by the NOAA-11 satellite, 10–12 April 1989; b) the North Wall of the Gulf Stream found by the procedure after the first opening and closing operation; c) eddies found by the procedure after the second opening and closing operation; d) the North Wall and warm-core eddies found by a human analyst (red) and by another automated procedure (green).

not interpolate where edge sections are obscured. Figure 4c shows eddies found. The warm-core eddies are found well, but a large amount of unwanted cloud cover is found by the procedure as well. Figure 4d shows the North Wall and one warm-core eddy found by a human analyst and by the other automated technique.

Figure 5a shows an inverted composite image from 21–23 April 1989. This image is fairly typical in its amount of cloud cover. Figure 5b shows the North Wall found. Again, it is clear except where clouds actually cover the edge. The North Wall found agrees more closely with that indicated by the human analyst in Figure 5d than does the

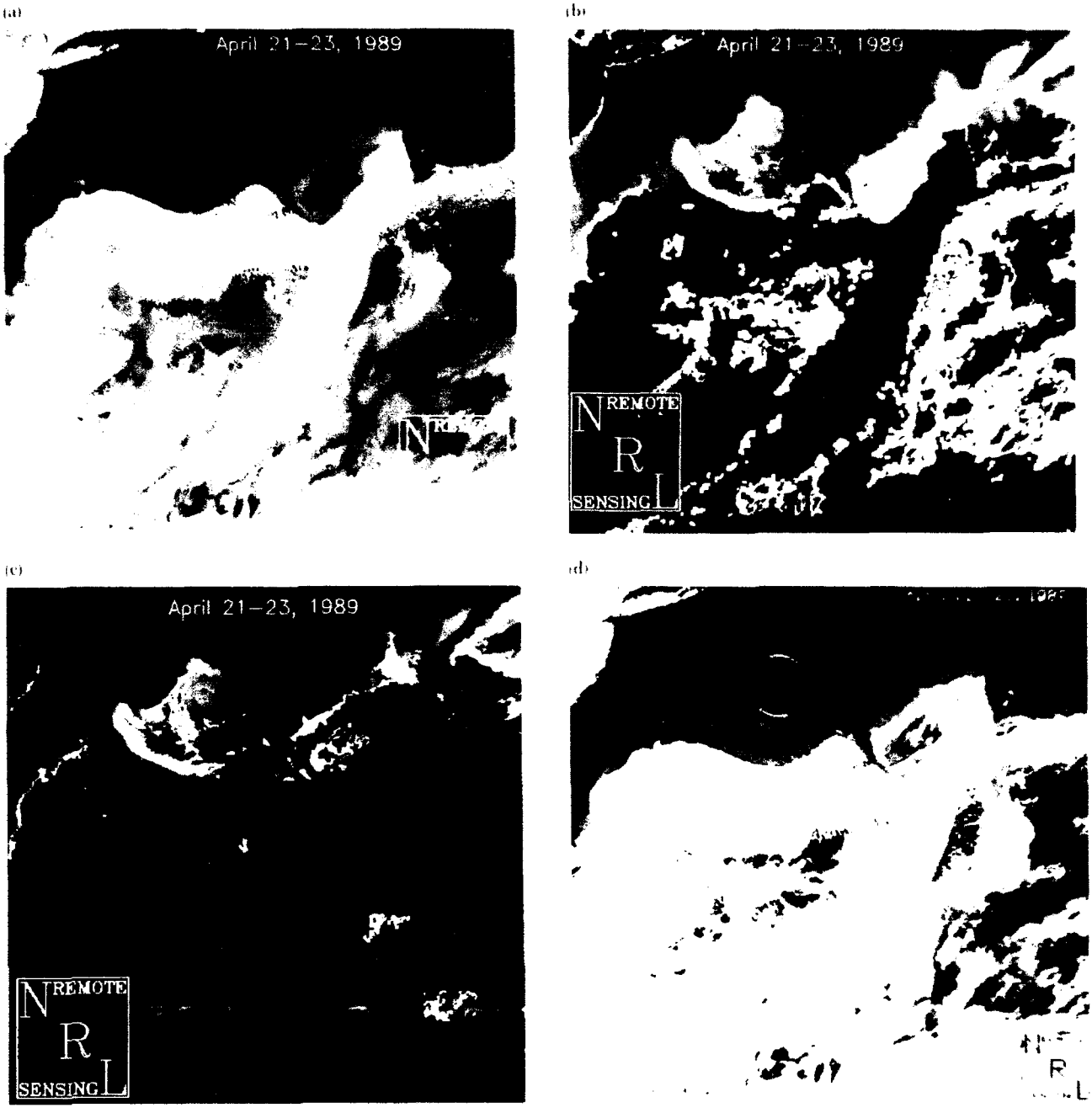

Figure 5. All images are displayed using histogram equalization to enhance the contrast. (a) An inverted warmest pixel composite of images acquired by the NOAA 11 satellite, 21–23 April 1989, by the North Wall of the Gulf Stream found by the procedure after the first opening and closing operation. (c) eddies found by the procedure after the second opening and closing operation. (d) the North Wall and warm-core eddies found by a human analyst, red, and by another automated procedure, green.

wall found by the other automated procedure (also shown in Fig. 5d). Figure 5c shows the eddies found. Again, warm-core eddies are found well. With a slight change in thresholds, two cold-core eddies south of the Gulf Stream also become visible, but at the cost of considerably more unwanted water. Traces of the cold eddies are visible in the image shown as Figure 5c.

The performance of the procedure on cold-core eddies is not good, because these eddies look less like stars in the inverted images used. Consequently, a test of using the original unin-

Figure 6. Eddies found using an uninverted version of Figure 5a. The threshold used was specialized to the image. The image is displayed using histogram equalization to enhance the contrast.

verted) images to find cold-core eddies was made. Figure 6 shows the results for the image of 21–23 April. The cold-core eddies are found by the procedure in this test; however, since they match the water around them closely in temperature, large amounts of this water are found in addition. Work is in progress on developing a general method to find both warm-core and cold-core eddies.

SUMMARY

The method finds the North Wall of the Gulf Stream in approximately the same place as human analysts and another automated procedure, generally better than the latter. Warm-core eddies are found as well by this method as by the other methods. A major advantage of this method is that the edges found are continuous unless interrupted by cloud cover. The edges are also sharp: Border pixels are all of zero intensity. However, when eddies are associated with trails of water of approximately the same temperature, the method does not separate eddies from trails. It also finds some unwanted land areas and cloud cover. It should be noted, however, that no shape information has been included to discriminate between eddies and trails, nor between eddies and unwanted objects; also, no "masking" of land or clouds was used.

The performance of the method on cold-core eddies is not good, primarily because cold-core eddies do not resemble stars as closely as do warm-core eddies. We can improve the performance on cold-core eddies by using techniques which make them look more like stars.

We conclude that this method shows promise of being useful in conjunction with other portions of the automated system, which complement its weaknesses nicely.

This work was partially sponsored by the Office of Naval Technology under PE 0602435N, CDR Lee Bounds, Program Manager. The authors are happy to thank S. Peckinpaugh for providing imagery and the results of other analyses, B. Grant for image processing support, and J. Hawkins for useful suggestions about the text. We also thank an anonymous referee for suggestions which materially improved the presentation in this paper. This document is approved for public release, distribution is unlimited. This is NRL Contribution JA 321-047-92.

REFERENCES

Buckles, B. P., and Petry, F. E. (1991). Labelling North Atlantic mesoscale features from satellite photographs: a new approach. In *Proceedings: Automated Interpretation of Oceanographic Satellite Images Workshop* (M. Lybanon, Ed.). Naval Oceanographic and Atmospheric Research Laboratory, Stennis Space Center, MS. pp. 93–102.

Cambridge, V. (1991). Edge-region correlation in image segmentation and analysis. In *Proceedings: Automated Interpretation of Oceanographic Satellite Images Workshop* (M. Lybanon, Ed.). Naval Oceanographic and Atmospheric Research Laboratory, Stennis Space Center, MS. pp. 183–188.

Cayula, J.-F., Cornillon, P., Holyer, R., and Peckinpaugh, S. (1991). Comparative study of two recent edge-detection algorithms designed to process sea-surface temperature fields. *IEEE Trans. Geosci. Remote Sens.* GE-29(1) 175–177.

Coulter, R. E. (1983). Applications of the Bayes decision rule for an automatic water mass classification from satellite infrared data. In *Proceedings 17th International Symposium on Remote Sensing of the Environment*. Vol. II. Environmental Research Institute of Michigan, Ann Arbor, MI. pp. 589–597.

Gerson, D. J., Khedouri, E., and Gaborski, P. (1982). Detecting the Gulf Stream from digital infrared data pattern recognition. In *The Belle W. Baruch Library in Marine Science, Vol. 12, Processes in Marine Remote Sensing*. Univ. of South Carolina Press, Columbia. pp. 19–39.

Haddon, J. F., and Boyce, J. F. (1990). Image segmentation by unifying region and boundary information. *IEEE Trans. Pattern Anal. Machine Intell.* PAMI-12(10):929–948.

Haralick, R. M. (1982). Pattern recognition of remotely sensed data. In *Pictorial Data Analysis* (R. M. Haralick, Ed.). Springer-Verlag, New York, pp. 351–367.

Haralick, R. M., Sternberg, S. R., and Zhuang, X. (1987). Image analysis using mathematical morphology. *IEEE Trans. Pattern Anal. Machine Intell.* PAMI-9(4):532–550.

Holyer, R., and Peckinpaugh, S. (1989). Edge detection applied to satellite imagery of the oceans. *IEEE Trans. Geosci. Remote Sens.* GE-27(1):46–56.

Janowitz, M. F. (1985). Automatic detection of Gulf Stream rings. Office of Naval Research Tech. Rep. TR-JS501.

Krishnakumar, N., and Iyengar, S. S. (1991). A hybrid technique for interpreting mesoscale analysis system (SAMAS). In *Proceedings: Automated Interpretation of Oceanographic Satellite Images Workshop* (M. Lybanon, Ed.). Naval Oceanographic and Atmospheric Research Laboratory, Stennis Space Center, MS, pp. 37–48.

Krishnakumar, N., Iyengar, S. S., Holyer, R., and Lybanon, M. (1990). An expert system for interpreting mesoscale features in oceanographic satellite images. *Int. J. Pattern Recognition Artific. Intell.* 4:341–355.

Lea, S. M. (1991). Finding ocean structure using mathematical morphology. In *Proceedings: Automated Interpretation of Oceanographic Satellite Images Workshop* (M. Lybanon, Ed.). Naval Oceanographic and Atmospheric Research Laboratory, Stennis Space Center, MS, 189–200.

Lea, S. M., and Kellar, L. A. (1989). An algorithm to smooth and find objects in astronomical images. *Astron. J.* 97: 1238–1246 (and plates on pp. 1269–1276); erratum (figures reversed), *Astron. J.* 98:736.

Lybanon, M., and Thompson, J. D. (1991). The role of expert systems in ocean forecasting. In *Conference Proceedings, MTS '91*, New Orleans, 10–14 November 1991. Marine Technology Society, Washington, DC, pp. 1137–1143.

Lybanon, M., McKendrick, J. D., Blake, R. E., Cockett, J. R. B., and Thomason, M. G. (1986). A prototype knowledge-based system to aid the oceanographic image analyst. In *Applications of Artificial Intelligence III*, SPIE 635, Bellingham, WA, pp. 203–206.

Lybanon, M., Peckinpaugh, S., Holyer, R., and Cambridge, V. (1990). Integrated ocean understanding system. *Image Understanding in the '90s: Building Systems that Work*, SPIE 1406, Bellingham, WA, pp. 180–189.

Molinelli, E. J., and Flanigan, M. J. (1987). Optimized CEOF interpolation of the Gulf Stream. Tech. Rep. TR-892395, Planning Systems, Inc., McLean, VA.

Molinelli, E. J., Muncill, G., and Pepe, K. (1991). Progress with neural network Gulf Streams. In *Proceedings: Automated Interpretation of Oceanographic Satellite Images Workshop* (M. Lybanon, Ed.). Naval Oceanographic and Atmospheric Research Laboratory, Stennis Space Center, MS, pp. 103–132.

Nichol, D. G. (1987). Autonomous extraction of an eddy-like structure from infrared images of the ocean. *IEEE Trans. Geosci. Remote Sens.* GE-25:28–34.

Peckinpaugh, S. H., and Holyer, R. J. (1991). Edge detection applied to infrared images of the ocean. In *Proceedings: Automated Interpretation of Oceanographic Satellite Images Workshop* (M. Lybanon, Ed.). Naval Oceanographic and Atmospheric Research Laboratory, Stennis Space Center, MS, pp. 9–36.

Serra, J. (1982). The hit or miss transformation, erosion and opening. In *Image Analysis and Mathematical Morphology*. Academic, New York, pp. 34–62.

Szczechowski, C. (1991). The Marr-Hildreth operator as an eddy detector. In *Proceedings: Automated Interpretation of Oceanographic Satellite Images Workshop* (M. Lybanon, Ed.). Naval Oceanographic and Atmospheric Research Laboratory, Stennis Space Center, MS, pp. 153–168.

Wilson, S. S. (1989). Vector morphology and iconic neural networks. *IEEE Trans. Syst. Man Cybernet.* SMC-19(6): 1636–1644.